nature portfolio

Peer Review File

Day/Night imaging without Infrared Cutfilter Removal based on metal-gradient perovskite single crystal photodetector

REVIEWER COMMENTS

Reviewer #1 (Remarks to the Author):

The paper entitled "Day/Night imaging without Infrared Cutfilter Removal based on metal-gradient perovskite single crystal photodetector" investigates the concept of utilizing a composition gradient to facilitate a variable-spectrum response under different biases, an interesting and intriguing approach. It demonstrates that binary lead-tin (PbSn) perovskites could be effectively employed in this context, potentially advancing the development of imaging sensors with high color fidelity and a large dynamic range (LDR). However, to fully realize the potential of this concept and its applicability in the field, a more comprehensive understanding of the underlying mechanisms and design principles is crucial. While the initial premise is engaging, the manuscript falls short in terms of clear presentation and interpretation of data, necessitating substantial revisions before its consideration for publication in Nature Communications. My critique is focused specifically on Figure 3, a central element of the paper, which I believe requires particular attention to detail and clarity.
- The assessment of penetration depth requires analysis of both the absorption spectra with absolute numbers for the coefficients. Given the typically greater penetration depth of infrared light compared to visible light (due to the lower absorption coefficient, referenced in Figure 1e), the current depiction in Figure 3a appears misleading and needs revision for accuracy.
- The manuscript indicates that under a -3V bias, the tin-rich region absorbs a significant portion of infrared light (with an External Quantum Efficiency (EQE) of 40%). Considering the lower absorption coefficient at wavelengths >850 nm, it is reasonable to infer near-complete absorption (over 90%) of light at 700 nm by the tin-rich area, thereby preventing its reach to the lead-rich region. Addressing this discrepancy might involve simulating light propagation using software like COMSOL to accurately determine absorption locations across varying wavelengths.
- When disregarding the gradient and focusing solely on light penetration depth across the spectrum, the possibility of a variable-spectrum response under different biases due to deeper penetration of longer wavelengths emerges. The manuscript should critically evaluate the necessity and benefits of the gradient strategy over a uniform binary lead-tin film without gradient. It is best to show the results of the devices using uniform Pb-Sn film.
- The observation of an EQE exceeding 140% in Figure S23 suggests that the device operates on a photoconductive mechanism rather than a photovoltaic one. This has profound implications, particularly considering the potential gradient in charge carrier mobilities across the film. A detailed discussion on the impact of mobility gradient in the context of photoconductance is needed.
- The conclusion of a light-induced injection mechanism needs stronger justification. The referenced literature (Ref 46) describes a distinct architecture operational in the UV range (high energy to overcome the injection barrier), which may not correlate with infrared detection in the absence of transport layers. The manuscript should address these discrepancies and provide a more coherent rationale.
- The observed rectification in dark current, in the absence of a transport layer, implies differing contacts between the film and electrodes at two sides. This aspect is critical and should be thoroughly explored, especially in the context of the dark and photo-response mechanisms.
- The recertification side gets reversed with light illumination. How author explain this observation?
- Figure 3d is unclear and lacks informative value. Clarification on carrier movement under flat band conditions for both dark and illuminated scenarios is needed.

- The manuscript posits band bending at the perovskite interface with contacts as a source of the light response. This hypothesis requires elaboration, especially in terms of how absorption location influences this effect. Additionally, if the holes are trapped, how we can exclude the possibility if recirculation of electrons across the device and generation of gain mechanism?
- The methodology for measuring the dynamic range, particularly under infrared light and at different biases (-1V vs. -3V), should be clearly defined, given the paper's focus on infrared detection.

Reviewer #2 (Remarks to the Author):

In the manuscript “Day/Night imaging without Infrared Cutfilter Removal based on metal-gradient perovskite single crystal photodetector”, the authors develop variable-spectrum responsive photodetectors based on Pb-Sn alloyed perovskite single crystals with vertical bandgap gradients. Through a combination of material characteristics and theory calculations, they demonstrate the oxygen exposure in favor of replacing Pb with Sn and correlate these compositional gradients to the underlying interactions between Sn perovskite and oxygen. However,
1. the response range of voltage regulation is no longer a unique concept (ACS Appl. Mater. Interfaces 2020, 12, 43).
2. Multi band responsive detectors (visible and infrared bands) have been widely reported.
3. Although this article proposes switchable responses, the extracted optical signal dimensions are still limited (only intensity signals). Unable to replace the current spectrometer. Therefore, the application scenarios of this detector still need to be discussed.
4. No significant advantages of perovskite single crystals compared to other materials were found in the article. Why does the author have to use perovskite single crystals? Can perovskite thin films achieve similar functions?
5. The author mentioned that integrating multiple materials with different bandgaps to achieve spectral analysis is complex. However, to my understanding, the material preparation in some articles is very simple (Adv. Mater. 2020, 32, 1908108. Science 365, 1017–1020 (2019)).
6. Current computational spectral analysis equipment has overcome the limitation of integrating multiple materials. In situ voltage regulation of light response further reduces the spectral analysis capability and footprint of the computational spectrometer (A wavelength-scale black phosphorus spectrometer. Broadband miniaturized spectrometers with a van der Waals tunnel diode. Miniaturized spectrometers with a tunable van der Waals junction). Therefore, this manuscript cannot be recommended for publication.

Reviewer #3 (Remarks to the Author):

The manuscript of Ma et al. describes an interesting study on conductive photodetectors made from Pb-Sn perovskites that show a voltage-dependent spectral response spectrum. This enables constructing detectors that are sensitive to different colors under different bias conditions and could simplify color imaging. There are a few concerns that the author should address in my view, especially regarding the mechanism they propose.

1. The text on lines 75-77 is very vague and difficult to understand. This should be clarified.

2. Lines 221-227. Pb-Sn based perovskites usually have a lower absorption coefficient than

pure Pb based perovskites, especially in the long wavelength region. For both perovskites the extinction coefficient increases towards shorter. Hence, short wavelengths are absorbed near the top surface and long wavelengths have larger penetration depth. This is exactly opposite to what the authors write. Hence, I have difficulty in understanding the mechanism shown in Figure 3a that should explain the bias dependence of the spectral response. The authors should explain why the penetration depth of short wavelength light is longer.

2. A key factor of the proposed mechanism is the fact that electrons are unable to drift across the entire crystal. Yet on lines 273-273 the authors argue that the electron mobility is very high and even 10-fold higher than the hole mobility. That raises the question of why electron transport is limiting the performance.

3. If this is a purely photoconductive detector, why then is the current under forward bias (Fig 3c) so much lower? What happens to the EQE spectrum under forward bias? If electron drift is limiting, should the relative sensitivity for UV and NIR light not switch under forward bias?

4. The LDR is claimed to be 177 dB. But Fig. 4b clearly shows a roll-off at the highest intensities. A double logarithmic plot hides many of the nonlinearities. It is better to make a semi-logarithmic plot of the ratio of the current and the light intensity versus the log of the light intensity. That should give a horizontal line and any deviation from that is the end of the LDR.

5. The time and fall times are relative long. A Si detector is much faster, does that have any consequences for the envisioned applications. Also in Fig. 4e it would be good to also indicate where state-of-the art perovskite photodiodes are positioned. I think LDRs will be similar and rise times well below 1 microsecond.

6. A minor issue: In the introduction the authors argue that application of existing ICR devices may be limited by insufficient long-term reliability under harsh conditions. The authors do not compare their single-crystal photodetectors to this statement.

Reviewers' Comments:

Reviewer #1 (Remarks to the Author):

The paper entitled "Day/Night imaging without Infrared Cutfilter Removal based on metal-gradient perovskite single crystal photodetector" investigates the concept of utilizing a composition gradient to facilitate a variable-spectrum response under different biases, an interesting and intriguing approach. It demonstrates that binary lead-tin (Pb-Sn) perovskites could be effectively employed in this context, potentially advancing the development of imaging sensors with high color fidelity and a large dynamic range (LDR). However, to fully realize the potential of this concept and its applicability in the field, a more comprehensive understanding of the underlying mechanisms and design principles is crucial. While the initial premise is engaging, the manuscript falls short in terms of clear presentation and interpretation of data, necessitating substantial revisions before its consideration for publication in Nature Communications. My critique is focused specifically on Figure 3, a central element of the paper, which I believe requires particular attention to detail and clarity.

1. The assessment of penetration depth requires analysis of both the absorption spectra with absolute numbers for the coefficients. Given the typically greater penetration depth of infrared light compared to visible light (due to the lower absorption coefficient, referenced in Figure 1e), the current depiction in Figure 3a appears misleading and needs revision for accuracy.

Our response: We apologize for the unclearness of Figure 3a. We have modified the scheme of Figure 3a. Following the suggestion from the Referee, we conducted optical research on the absorption coefficients of the perovskite materials. Due to the gradient metal distribution from the upper surface to the deep interior, we simulated the perovskite compositions by investigating the absorption coefficients of different perovskite films with various Pb:Sn ratios. As shown in the Figure R1a, the shoulder peak in the infrared light red-shifted as the ratio of Sn increase, but showed similar coefficients with slightly decreased intensity. It is worth noting that the perovskite single crystal has a red-shift absorption edge than its polycrystalline counterparts *(Nat. Commun.* **2017**, *8*, 1890). Figure 1e exhibits the red-shift absorption edge close to 1100 nm, which was hereinafter referred to calculate the absorption coefficient at wavelengths >850 nm.

Think of an optically thick layer as a bunch of optically thin layers all stacked together. In each optically thin layer, the change in radiation intensity, dI, is simply equal to the intensity coming in times the optical depth of that layer:

$$\mathrm{d}I = -(I)(n\sigma \mathrm{d}L) = -I\mathrm{d}\tau$$

where n is the number density of absorbers, L is the length of absorbers, and σ is the cross-section of the absorbers. So, we have the following differential equation:

$$\frac{\mathrm{d}I}{I} = -\mathrm{d}\tau$$

We integrate this from I_{in} to I_{out}:

$$\int_{I_{in}}^{I_{out}} \frac{\mathrm{d}I}{I} = -\int_{0}^{\tau} \mathrm{d}\tau$$

On the assumption that the shoulder peak appears on a linear move as the change of Pb:Sn ratio, the peak position follows the depth profiling derived from TOF-SIMS results. Taking the second response peak at

940 nm, for example, the calculated maximum absorbance portion of infrared light within the Sn-rich region (100 nm) was around 8%. In contrast, the absorbance portion of light at 700 nm was calculated as ~28%.

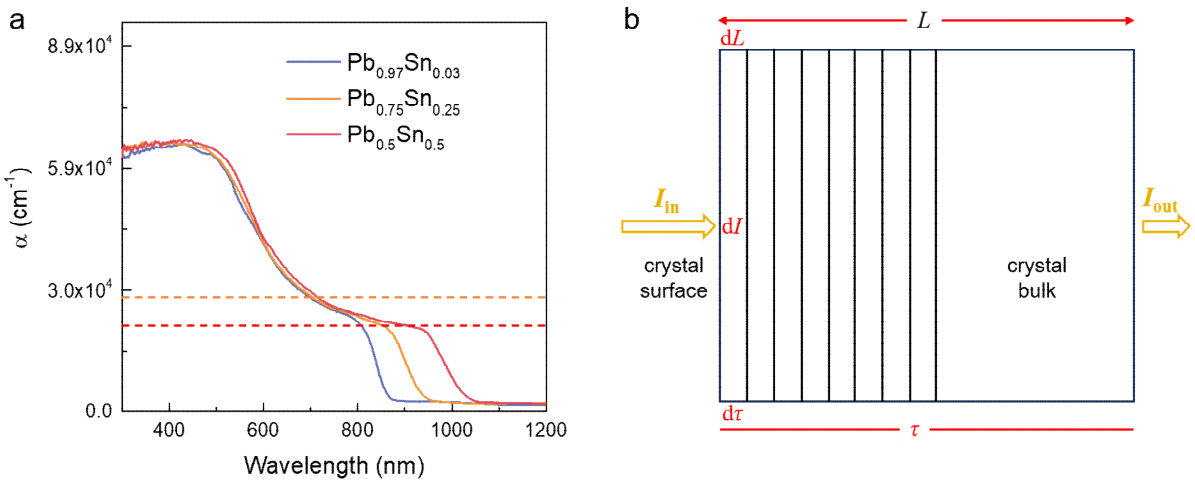

Figure R1. a) The calculated absorption coefficient curve of Pb-Sn mixed perovskite films with different Pb:Sn ratios. b) Schematic illustration of optical depth in the stacked absorbers.

2. The manuscript indicates that under a -3V bias, the tin-rich region absorbs a significant portion of infrared light (with an External Quantum Efficiency (EQE) of 40%). Considering the lower absorption coefficient at wavelengths >850 nm, it is reasonable to infer near-complete absorption (over 90%) of light at 700 nm by the tin-rich area, thereby preventing its reach to the lead-rich region. Addressing this discrepancy might involve simulating light propagation using software like COMSOL to accurately determine absorption locations across varying wavelengths.

Our response: As noted by the reviewer, the absorption coefficient of the material is higher in the visible than in the infrared. However, the thickness of the Sn-rich layer in this work is very thin, determined by TOF-SIMS results (around 100 nm thick). Owing to that the trap-induced injection mechanism has a multiplier effect on EQE, the infrared EQE obtained at −3 V bias cannot directly represent the absorption ratio of infrared light. As shown in the discussion above, the Sn-rich perovskite region on the surface does not completely absorb all visible light, let alone infrared light. Most visible light can penetrate the Sn-rich region and reach the bulk, and therefore, the short-wave and long-wave photo-generated carriers have different spatial distributions.

Following the reviewer's recommendations, we simulated the propagation of light through the material. We selected 750 nm and 940 nm light as the characteristic wavelength to analyze the generation position of short-wavelength and long-wavelength photo-generated carriers, respectively. For the gradient distribution of Sn at the surface, we simplified the process by dividing the 100 nm surface into five regions with different optical constants. In order to approach the actual situation as closely as possible, the optical constants were measured from the perovskite film with the same Pb:Sn ratio of the Sn-rich region derived from the TOF-SIMS results. The model of the material is shown in Figure R2a. The thickness of the first five regions was set to 20 nm, and the bulk region (Region 6) was set to 900 nm.

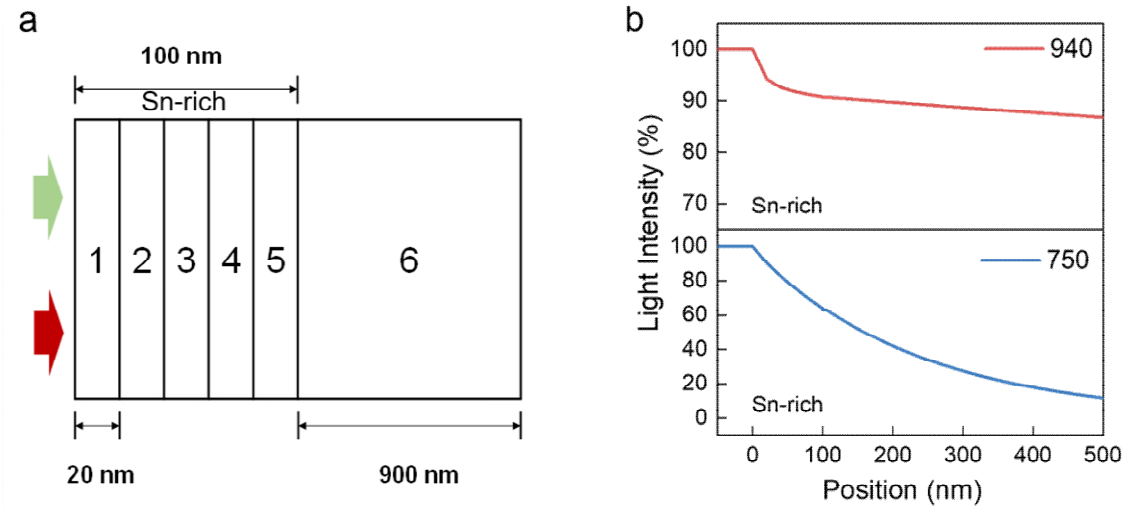

Figure R2. (a) Material model for optical simulation. Regions 1-5 are surface Sn-rich regions with a thickness of 20 nm for each region. Region 6 is the bulk region with a thickness of 900 nm. (b) Optical simulation results for propagation depths of 940 nm and 750 nm light.

The simulation results are shown in Figure R2b. The long-wavelength infrared light of 940 nm is mainly absorbed by the Sn-rich region of the first 100 nm, with negligible absorption in the bulk region. In contrast, the absorption of short-wavelength visible light of 750 nm exists in the whole material model. Therefore, the long-wavelength photogenerated carriers are mainly distributed in the Sn-rich region, while the short-wavelength photogenerated carriers are distributed across the entire material. The spatial distribution of spectral responses provides the platform to present variable-spectrum responses at different biases. The optical constants of each region are shown in Table R1.

Table R1. The optical constants of each region under 750 nm and 940 nm light.

Region	n_{940}	k_{940}	n_{750}	k_{750}
1	2.41634	0.20272	2.41193	0.27375
2	2.14785	0.06507	2.17927	0.25975
3	2.08465	0.03267	2.12452	0.25645
4	2.06432	0.02225	2.10689	0.25539
5	2.05738	0.01869	2.10088	0.25503
6	2.05514	0.01257	2.09894	0.25491

3. When disregarding the gradient and focusing solely on light penetration depth across the spectrum, the possibility of a variable-spectrum response under different biases due to deeper penetration of longer wavelengths emerges. The manuscript should critically evaluate the necessity and benefits of the gradient strategy over a uniform binary lead-tin film without gradient. It is best to show the results of the devices using uniform Pb-Sn film.

Our response: We are grateful to the Referee for this suggestion. The gradient doping of Sn makes the perovskite on the surface present a composition gradient change; that is, it brings a curved band structure, which is conducive to the separation of carriers. The separation reduces the recombination probability of non-equilibrium carriers and improves the carrier collection efficiency of electrodes. The same energy band structure and carrier separation promotion were obtained by epitaxial growth of the single crystal with Sn composition gradient in other research (*Nature* **2020**, *583*, 790–795).

Because Sn gradient distribution naturally appears in the crystal growth of this work, we study the influence by analyzing tin-lead thin films. According to the method reported in references (*Adv. Mater.* **2022**, *34*, 210772; *Small* **2023**, *19*, 2205976), we fabricated two samples with different Sn distributions (gradient and uniform) by adjusting the process conditions such as antisolvent temperature. Transient absorption spectra (TAS) of samples with different Sn distributions were studied by excitation with a 515 nm femtosecond laser. The dynamic analysis of the TAS, as shown in Figure R3, shows that the ground state bleaching (GSB) signal lifetime at 940 nm of the sample with Sn gradient distribution is much longer. It indicates that the Sn gradient promotes the separation of photogenerated carriers and suppresses the recombination of non-equilibrium carriers, which is consistent with our discussion.

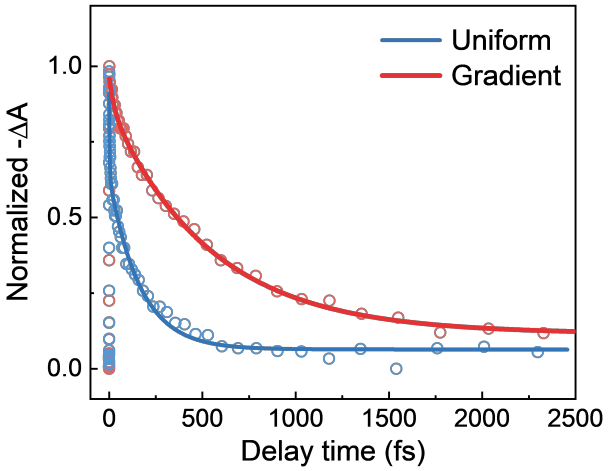

Figure R3. TAS kinetic analysis of uniform and gradient Sn distribution samples. The fitting lifetimes of the uniform and gradient distribution thin-film samples are 163 and 537 ps, respectively.

4. The observation of an EQE exceeding 140% in Figure S23 suggests that the device operates on a photoconductive mechanism rather than a photovoltaic one. This has profound implications, particularly considering the potential gradient in charge carrier mobilities across the film. A detailed discussion on the impact of mobility gradient in the context of photoconductance is needed.

Our response: As mentioned by the reviewer, an EQE exceeding 100% indicates that the device is not operating on the photovoltaic mechanism. The detailed EQE gain mechanism of the perovskite devices has

been provided in our response to Question 9. We believe that the main source of EQE gain is the trap-induced injection mechanism that disables the barrier. Theoretically, the difference in electron and hole mobility would hardly have a huge impact on the gain in the photoconductive mechanism since the Schottky barrier limits electron recruitment from the external circuit.

Although we believe that the mobility difference contributes little to the gain effect of the device, the potential gradient caused by the Sn gradient distribution significantly enhances carrier separation and transport. This makes collecting photo-generated carriers more efficient for devices operating in the photoconductive mechanism, especially for photo-generated electrons and external circuit replenishment electrons. The influence of tin gradient distribution on charge transport in photoconductive was simulated by using the same process as reported above to produce lead-tin perovskite thin films with ITO and copper as electrodes. By irradiating a 365nm nanosecond laser on the device, the transient photocurrent (TPC) lifetime can be studied to investigate the carrier transport characteristics of devices operating in photoconductive mode. As shown in Figure R4, the TPC lifetime of the uniform device is 11.8 μs, while that of the gradient device is 4.4 μs. This indicates that under the action of an electric field, the gradient distribution of tin contributes to the drift of photo-generated carriers.

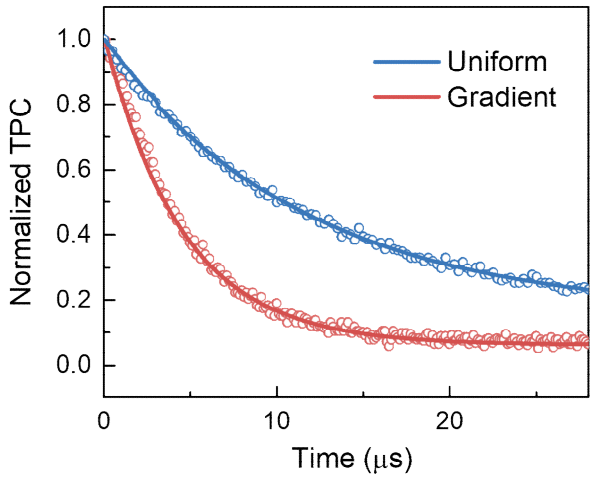

Figure R4. TPC fitting lifetime of uniform and gradient Pb-Sn perovskite devices.

5. The conclusion of a light-induced injection mechanism needs stronger justification. The referenced literature (Ref 46) describes a distinct architecture operational in the UV range (high energy to overcome the injection barrier), which may not correlate with infrared detection in the absence of transport layers. The manuscript should address these discrepancies and provide a more coherent rationale.

Our response: We thank the reviewer for the comment. The mechanism of trap-induced carrier injection is that holes trapped by trap states in the material result in band bending. In such a case, the width of the Schottky barrier is narrowed to improve the tunneling probability. Furthermore, the energy band position is lowered to provide empty states that can accommodate tunneling electrons, thus reducing the barrier effect on carrier injection under bias voltage. Based on the reviewer's suggestion in Question 8, we have redrawn Figure 3d to explain the trap-induced charge injection mechanism further.

Although Ref. 44 (*Nat. Nanotech.* **2012**, *7*, 798-802) describes a carrier-induced injection mechanism similar to that described in this paper, that is, ultraviolet photogenerated electrons in ZnO nanocomposite are trapped by potential barriers, thus inducing multiplication of hole injection in external circuits, its operating wavelength is misleading. Therefore, we replaced it with research on photodetectors in the infrared region (*Adv. Mater.* **2016**, *28*, 2043–2048).

6. The observed rectification in dark current, in the absence of a transport layer, implies differing contacts between the film and electrodes at two sides. This aspect is critical and should be thoroughly explored, especially in the context of the dark and photo-response mechanisms.

Our response: We agree with the Reviewer that there are differing contacts between the film and electrodes on two sides. The electrode materials of the photodetector are ITO and gallium, and the corresponding work functions are -4.7 and -4.2 eV, respectively. The reference result (*Nature* **2023**, *620*, 545–551) shows that the work function of ITO does not change significantly after contact with perovskite, and the existence of the Schottky barrier leads to the rectification phenomenon in the dark state. Lots of research reported that photodetectors constructed by electrodes with various work functions and perovskite single crystals produced a rectification effect. (*Nat. Photon.* **2024**, *18*, 250–257; *Nat. Photon.* **2015**, *9*, 679–686) Under illumination, the Schottky barrier will promote the collection of carriers. (*Adv. Funct. Mater.* **2023**, *33*, 2306526; *Matter* **2019**, *1*, 639–649; *Adv. Funct. Mater.* **2023**, *33*, 2302175) To further illustrate the effect of electrode contact on the photodetector, we supplemented references and added the EQE results measured under zero bias. As shown in Figure R5, the device can still separate the photo-generated carrier to obtain a photo response without external bias voltage.

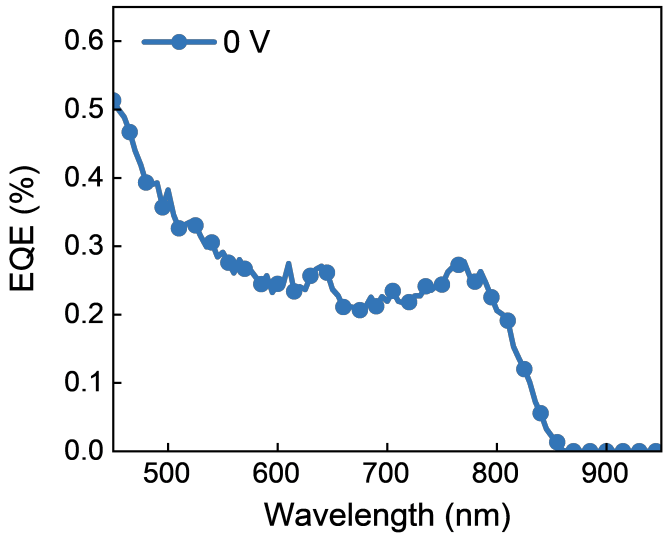

Figure R5. EQE results of the perovskite single crystal photodetector measured at 0 V bias.

7. The recertification side gets reversed with light illumination. How author explain this observation?

Our response: As mentioned in our response to Question 6, Schottky barriers in the device introduce a rectification effect that lowers the dark currents at negative voltages. However, the Schottky barrier fails to

hinder carrier injection when trap-induced carrier injection occurs under illumination. In such a case, we can obtain photocurrent under multiplication, reversing rectification characteristics. This phenomenon has been widely reported in the references of photodetectors. (*Nat. Nanotech.* **2012**, *7*, 798-802; *Sci. Adv.* **2020**, *6*, eaaw8065) Admittedly, holes need to drift to the counter electrode at positive voltages, and thus, a lower hole mobility can also affect photocurrent.

8. Figure 3d is unclear and lacks informative value. Clarification on carrier movement under flat band conditions for both dark and illuminated scenarios is needed.

Our response: We agree with the Referee that our illustration in the previous version was not clear. To better explain the trap-induced charge injection mechanism, we have redrawn Figure R6. We have updated Figure 3d in the revised manuscript.

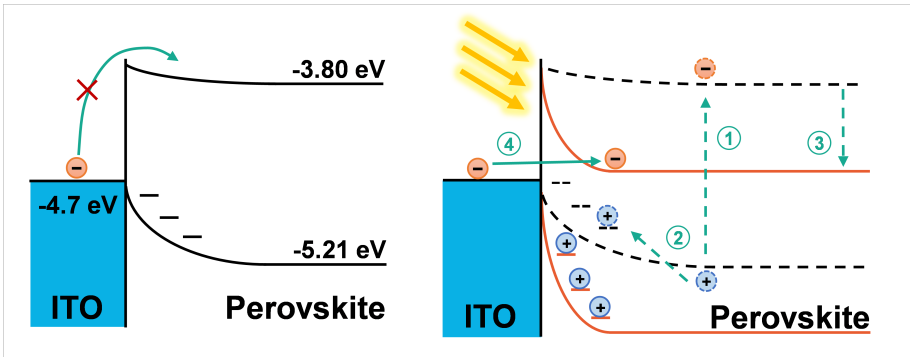

Figure R6. Schematics of the energy band structure under dark and illumination. In the dark, the external electrons are blocked by the Schottky barrier, while the trap-induced charge injection mechanism under illumination can be divided into four steps: 1) electron-hole pair generation; 2) hole trapping process; 3) band bending and barrier narrowing; 4) electron tunneling process.

9. The manuscript posits band bending at the perovskite interface with contacts as a source of the light response. This hypothesis requires elaboration, especially in terms of how absorption location influences this effect. Additionally, if the holes are trapped, how we can exclude the possibility if recirculation of electrons across the device and generation of gain mechanism?

Our response: Following the suggestions from the Referee, we have redrawn Figures 3a and 3d and provided a detailed explanation of the source of the light response. According to the work function of contact electrodes and the band structure of perovskite, there are two band bends in perovskite materials. The band bending on the gallium electrode side is caused only by electrode contact, while the band bending on the ITO side is caused by electrode contact and Sn gradient doping. For short-wavelength light, the source of the photo response is in the region of light absorption from the ITO side to the interior. For long-wavelength light, only the band bending area under ITO can absorb and form a light response because the bulk perovskite component cannot absorb.

In the pure photoconductive effect of ohmic contacts between symmetrical electrodes, the extraction and replenishment cycle of the other carrier in the device can produce gain when one carrier is trapped. However, the current-voltage curves of the photodetectors in this work indicate that Schottky barriers exist, not pure ohmic contacts. Therefore, if the trap-induced injection mechanism is not considered, the holes are trapped,

and the electrons are extracted from the device. However, the electrons of the external circuit are blocked by Schottky barriers, so the tunneling probability is very low, and it cannot be effectively supplemented by the device to form a cycle. Thus, we can theoretically rule out the possibility that electron cycles play a dominant role in the gain mechanism. As mentioned in the response to the previous question, the trap-induced injection mechanism can greatly improve the tunneling mechanism of electrons, which can form considerable gains.

10. The methodology for measuring the dynamic range, particularly under infrared light and at different biases (-1V vs. -3V), should be clearly defined, given the paper's focus on infrared detection.

Our response: Thanks to the reviewer's suggestion, we added details of dynamic range measurements to the method. In addition, according to the reviewer's comments, the linear dynamic range of 940 nm infrared light at −3 V was added to the supplementary information (Figure R7). The LDR measured at −3 V under 940 nm light irradiation is also >170 dB, consistent with that of visible light.

The detailed methodology for LDR measurement has been added in the revised manuscript. 635 nm and 940 nm lasers were used as the light source, and the extensive range of light intensity was achieved by combining five neutral density filters with optical density values of 0.5, 1, 2, 3, and 4. Keysight B2901A sourcemeter was used to record the photocurrent of the photodetector. The optical power was verified using the Newport 843-R optical power meter. The photodetector operated at −1 and −3 V bias when tested under 635 and 940 nm laser illumination, respectively.

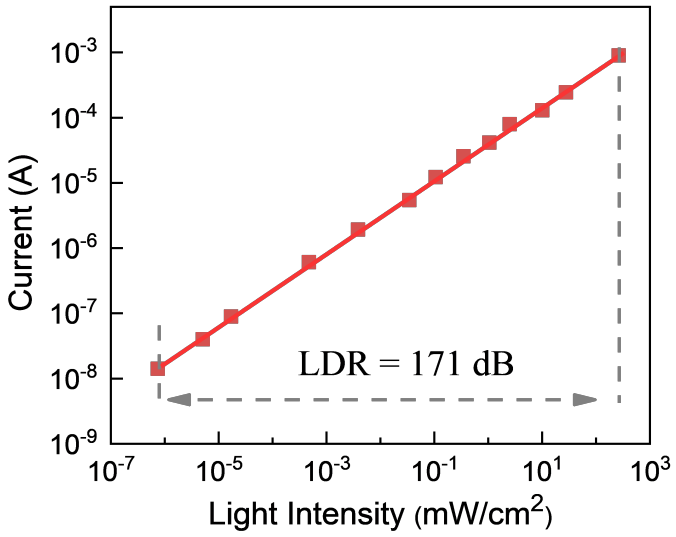

Figure R7. LDR of the perovskite photodetector measured at −3 V under 940 nm laser illumination.

Reviewer #2 (Remarks to the Author):

In the manuscript “Day/Night imaging without Infrared Cutfilter Removal based on metal-gradient perovskite single crystal photodetector”, the authors develop variable-spectrum responsive photodetectors based on Pb-Sn alloyed perovskite single crystals with vertical bandgap gradients. Through a combination of material characteristics and theory calculations, they demonstrate the oxygen exposure in favor of replacing Pb with Sn and correlate these compositional gradients to the underlying interactions between Sn perovskite and oxygen. However,

1. the response range of voltage regulation is no longer a unique concept (ACS Appl. Mater. Interfaces 2020, 12, 43).

Our response: We sincerely thank the Reviewer for taking the time to review the paper and for the feedback. However, we respectfully disagree on the novelty aspect. We would like to underline again that the key point of the paper is developing perovskite single crystal photodetectors for day/night imaging without ICR. To achieve this goal, two main obstacles, namely the preparation of a narrow-bandgap perovskite single crystal ($\leq$ 1.2 eV) and the realization of varying spectral responses, must be overcome.

We agree with the reviewer that previous works have been reported to realize the controllable switch in response to the bias voltage. Among those studies, many optimizations have been attempted to integrate multiple perovskite materials for the realization of multi-spectral responses. As mentioned by the Reviewer, the reference (*ACS Appl. Mater. Interfaces* **2020**, *12*, 48765-48772) reported dual-band photon detectors switched between 300−570 and 630−800 nm based on tandem configuration by using $MAPbBr_3$ and $MAPbI_3$ thin film as a photoactive layer for each subcell. However, such an approach requires complicated fabrication techniques with well-designed circuit designs to access separate materials. Alternatives, constructing multi-component bandgap gradient in a single perovskite activelayer provides an effective approach to regulate the optoelectronic properties (*Nano Res*. **2023**, *16*, 10256-10262; *Light Sci. Appl*. **2020**, *9*, 162). Nevertheless, the halide gradient (Cl, Br, and I) is basically the only option, as ever reported, to fine-tune the bandgap. Most halide gradients exhibit limited tunable direct bandgaps in the visible range (1.5–3.0 eV).

In this study, we proposed a strategy to achieve bandgap-gradient perovskite single crystal by B-site metal alloying. We elaborated on the principle of the Pb−Sn compositional gradient by underlying interactions between Sn perovskite and oxygen. This is the novelty of our manuscript, where we adopt the interactions to precisely regulate the vertical bandgap-graded structure, achieving a bias-switchable spectral response from visible to near-infrared region. Therefore, we disclose that the metal alloying of perovskite composition provides a platform for material design and functional integration. In addition, we focused on the preparation of perovskite single crystal rather than the perovskite film, which will be discussed in the following parts.

2. Multi band responsive detectors (visible and infrared bands) have been widely reported.

Our response: We agree with the reviewer that many optimizations have been attempted with spectrally selective detection to achieve multispectral perceptions. In our revised manuscript, representative works about multiband responsive detectors have been added in the Introduction part. In particular, visible- and infrared-selective photodetectors detectors have been investigated by using organic heterojunctions (*Sci. Adv.* **2020**, *6*, eaaw8065), quantum dot nanomaterials (*Nat. Photonics* **2019**, *13*, 277–282), and 2D materials

(*Sci. Adv.* **2021**,*17*, eabj2521). Taking the 2D materials, for example, fabricated van der Waals p-Ge/n-MoS2 heterojunction photodetector responds to dual-band spectrum by modulating the operation mode under different bias, which need complicated switching operation during multispectral detection. Moreover, the efficiency, response time, and responsibility still need to be further enhanced to meet the requirement of low crosstalk and high-resolution ratio (*Sci. Adv.* **2021**,*17*, eabj2521; *ACS Nano* **2018**, *12*, 8739; *Appl. Phys. Lett.* **2022**,*120*, 261101).

Until now, visible and infrared dual-band photodetectors relying on perovskite materials have been rarely reported. As shown in the reference (*ACS Appl. Mater. Interfaces* **2022**, *14*, 25824-25833), the perovskite composition engineering based on lead halide perovskite can only extend the response range around 850 nm, unacceptable for the demands of night imaging. Thus, how to design and prepare the narrow-bandgap perovskite single crystal ($\leq$ 1.2 eV) with multispectral response is still a technical challenge. Herein, for the first time, we adopt metal-gradient perovskite single crystal photodetectors to achieve a bias-switchable spectral response from visible to near-infrared region (close to 1100 nm) for day/night imaging.

3. Although this article proposes switchable responses, the extracted optical signal dimensions are still limited (only intensity signals). Unable to replace the current spectrometer. Therefore, the application scenarios of this detector still need to be discussed.

Our response: We think there might have been a misunderstanding on the Reviewer's side of application scenarios. The application of this perovskite single crystal photodetector is day/night imaging, not optical spectrometers. To reduce ambiguity, we have updated the Reference 14.

4. No significant advantages of perovskite single crystals compared to other materials were found in the article. Why does the author have to use perovskite single crystals? Can perovskite thin films achieve similar functions?

Our response: We thank the referee for this comment. Due to the simplicity of processing, perovskite electronic devices are heavily focused on thin polycrystalline films. Despite their advancements, perovskite thin films with a high density of structural defects (point defects, impurities, dislocations, and grain boundaries) face many challenges. On the contrary, perovskite single crystals exhibit a largely suppressed density of those structural defects due to the ordered lattice arrangement, which bestows several attractive benefits in optoelectronic performance and stability (Supplementary Figs. 22 and 36).

Optical Properties: Compared with polycrystalline thin films, the absorption range of perovskite single crystals is extended, which is attributed to the enhanced below-bandgap absorption and the clear band edge cutoffs with a small amount of in-gap defect states. The extended absorption range makes more photons absorbed.

Carrier dynamics: Trapped carriers are likely to be annihilated in deep trap states with large activation energies. The high trap density in the polycrystalline perovskite films leads to an increased non-radiative recombination of charge carriers, and thus, deteriorated device performance. In contrast, lower densities of structural defects and electronic traps in perovskite single crystals minimize the non-radiative recombination of charge carriers, as proven by the much-elongated carrier lifetime. (*Nat. Commun.* **2015**, *6*, 7586) Due to about six orders of magnitude lower defect density than their polycrystalline counterpart,

the best perovskite single crystals possess a large carrier lifetime of around hundreds of microseconds. (*Science* **2015**, *347*, 967)

Carrier mobility: Besides carrier trapping by forming deep electronic states, the point defects can also affect the carrier transport through the Coulomb-interaction-induced defect scattering. Thus, the point defects can alter the acceleration vector of the carriers. (Nat. Commun. 2017, 8, 590) Due to the reduced point defect densities and the weakened carrier phonon coupling, perovskite single crystals usually exhibit much enhanced carrier mobility. Furthermore, the absence of grain boundaries eradicates the possible scattering of the charge carriers, contributing to the excellent carrier dynamics in perovskite single crystals. (*Nat. Commun*. **2017**, *8*, 2230)

Ion migration: Due to the relatively low activation energy, ion migration is inevitable in polycrystalline perovskites films under an electric field during device operation. Due to the largely reduced densities of point defects and an absence of grain boundaries, the ion migration in perovskite single crystals would be significantly suppressed. As shown in the reference (*Phys. Chem. Chem. Phys*. **2016**, *18*, 30484–30490), the ion-migration activation energy in perovskite single crystals (1.05 eV) is significantly higher than that in polycrystalline halide perovskites (0.27–0.50 eV) under dark conditions.

Chemical Stability: The great merit of perovskite single crystals is their much-enhanced stability. Grain boundaries and defect sites can serve as the channel for moisture and oxygen penetration and gradually decompose the entire material. The low defect densities and absence of grain boundaries of perovskite single crystals lead to enhanced environmental stability (*Adv. Mater*. **2017**, *29*, 1602639). Similarly, the improvement of phase stability and the absence of ion migration results in enhanced stability against light and thermal treatment. (*Adv. Mater.* **2016**, *28*, 9204– 9209)

Operational stability: Due to the ion migration and potential electrochemical damage, the long-term operational stability is magnified under high electric bias. Single-crystal halide perovskites with low defect density show superiority in operational stability under a higher bias voltage. (*Nat. Commun.* **2020**, *11*, 274)

Overall, future studies of single-crystal halide perovskites represent a fertile ground for new breakthroughs in photodetector applications.

5. The author mentioned that integrating multiple materials with different bandgaps to achieve spectral analysis is complex. However, to my understanding, the material preparation in some articles is very simple (Adv. Mater. 2020, 32, 1908108. Science 365, 1017–1020 (2019)).

Our response: We apologize for the unclear information in lines 66-67. There are two approaches for achieving multispectral response: multisource (multijunction) and multiband (single-junction) photodetectors. For multisource photodetectors, we intended to express that the integration of individual VIS and IR photodetectors is limited by structural complexity. We have modified the expression in the introduction part.

6. Current computational spectral analysis equipment has overcome the limitation of integrating multiple materials. In situ voltage regulation of light response further reduces the spectral analysis capability and footprint of the computational spectrometer (A wavelength-scale black phosphorus spectrometer.

Broadband miniaturized spectrometers with a van der Waals tunnel diode. Miniaturized spectrometers with a tunable van der Waals junction). Therefore, this manuscript cannot be recommended for publication.

Our response: Again, we think there might have been a misunderstanding on the Reviewer's side of application scenarios. The application of this perovskite single crystal photodetector is day/night imaging, not optical spectrometers (Figure R8). The mentioned black phosphorus with a tunable van der Waals junction is applicable to spectrometer but not to imaging.

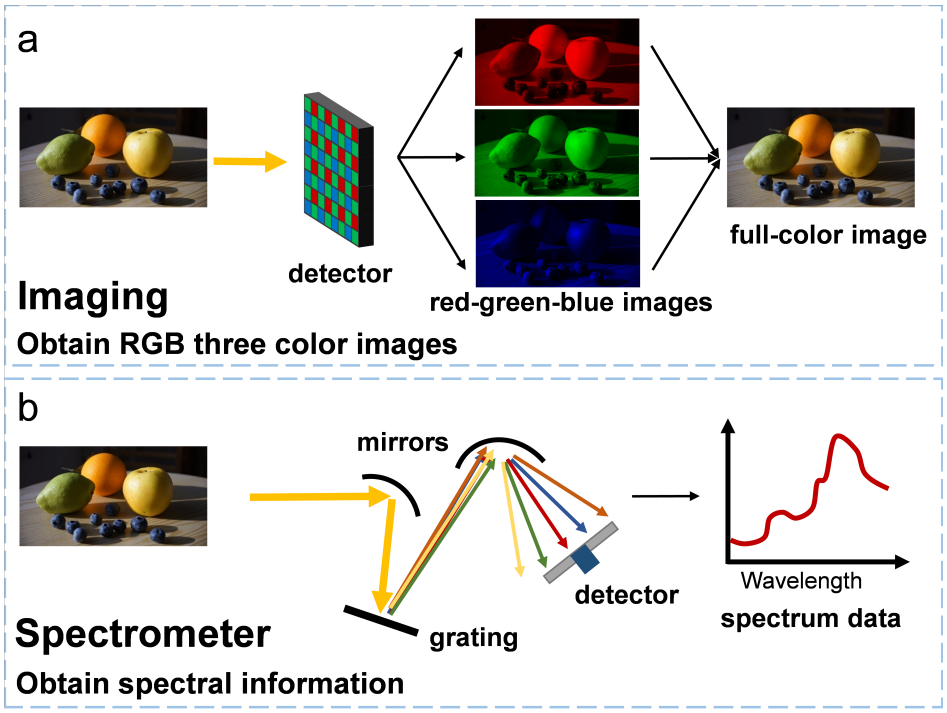

Figure R8. The difference between imaging and spectrometer. a) Imaging: obtain images of red, green, and blue colors through a detector array and then restore them to full-color images. In imaging applications, only three colors need to be distinguished without the need for wavelength resolution. b) Spectrometer: extracting wavelength information from light through various methods.

We agree with the Reviewer that current computational spectral analysis equipment has overcome the limitation of integrating multiple materials. However, in the field of day/night imaging, miniaturized devices without mechanical equipment are highly desirable for their application under harsh conditions, such as vehicle or drone cameras. The key significance of our work is that it demonstrates how the metal alloyed perovskite photodetectors allow a bias-switchable spectral response from visible to near-infrared region (close to 1100 nm). The large LDR (177 dB) and high grey-level resolution (over 26-bit) make it more widely available in day/night vision applications.

Therefore, we would argue against the comment that our work provides insufficient general interest for Nature Communications Readers.

Reviewer #3 (Remarks to the Author):The manuscript of Ma et al. describes an interesting study on conductive photodetectors made from Pb-Sn perovskites that show a voltage-dependent spectral response spectrum. This enables constructing detectors that are sensitive to different colors under different bias conditions and could simplify color imaging. There are a few concerns that the author should address in my view, especially regarding the mechanism they propose.

1. The text on lines 75-77 is very vague and difficult to understand. This should be clarified.

Our response: We apologize for being unclear. The text has been modified into “Through a combination of material characteristics and theory calculations, we demonstrate the effect of oxygen exposure on compositional gradients and elucidate the specific role of interactions between Sn perovskite and oxygen.”

2. Lines 221-227. Pb-Sn based perovskites usually have a lower absorption coefficient than pure Pb based perovskites, especially in the long wavelength region. For both perovskites the extinction coefficient increases towards shorter. Hence, short wavelengths are absorbed near the top surface and long wavelengths have larger penetration depth. This is exactly opposite to what the authors write. Hence, I have difficulty in understanding the mechanism shown in Figure 3a that should explain the bias dependence of the spectral response. The authors should explain why the penetration depth of short wavelength light is longer.

Our response: We agree with the reviewer's statement that Lambert-Beer law judges the depth of light penetration. In this work, the gradient distribution of Pb−Sn alloying presents Sn enrichment at the upper surface of the perovskite crystal with a very thin Sn-rich region (about 100 nm). Therefore, only the space within the surface could absorb the long-wavelength infrared light, but with a limited portion. Both long-wavelength light and short-wavelength light can penetrate this region, after which the long-wavelength light can no longer be absorbed within the bulk, while the short-wavelength light can continue to be absorbed, so there is a difference in the spatial distribution of photogenerated carriers. We describe the absorption of long-wavelength light on the surface and short-wavelength light throughout the material to highlight the generation position of long-wavelength photocarriers.

Based on the reviewer's comments, we realized that Figure 3a did not accurately represent our proposed mechanism, thereby we redrew Figure 3a. In contrast to the previous diagram, we describe the process of light absorption by narrowing the beam and demonstrate that long-wavelength light is not fully absorbed and transmitted to the bottom (Figure R9).

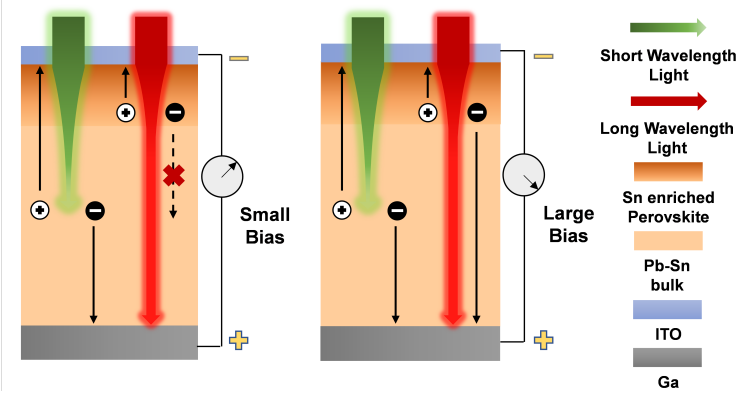

Figure R9. Schematics of the mechanism of variable-spectrum responsive photodetectors under different biases.

3. A key factor of the proposed mechanism is the fact that electrons are unable to drift across the entire crystal. Yet on lines 273-273 the authors argue that the electron mobility is very high and even 10-fold higher than the hole mobility. That raises the question of why electron transport is limiting the performance.

Our response: Thanks for the reviewer's question. In this work, the high electron mobility of the perovskite crystals is attributed to the tin incorporations and excellent crystal quality (*Nature* **2020**, *583*, 790–795; *Chem. Mater.* **2018**, *30*, 1556–1565). In contrast, the large number of hole traps introduced by the Sn enrichment led to a relatively low hole mobility.

Even though the electron mobility is much higher than the hole mobility, electrons cannot easily drift across the thick perovskite single crystals. As we know, the drift distance of carriers is related to mobility, lifetime, and bias voltage. Generally, the drift distance of electrons can be controlled by adjusting the bias voltage. Here, we showed that the long-wavelength photoelectrons generated on the surface cannot reach the counter electrode at low voltage but can be collected at high voltage. Specifically, we estimated the carrier diffusion and drift distance L at −1 V bias from the parameters reported in the reference (*Nat. Commun.* **2019**, *10*, 1066), where $\mu\tau$ is 1×10^{-2} cm^2/V:

$$L = \sqrt{\frac{k_B T}{q}\mu\tau} + \mu\tau\frac{V}{d} = \sqrt{0.0267 \times 1 \times 10^{-2}} + 1 \times 10^{-2} \times \frac{1}{0.15} = 0.083\ cm$$

where k_B is Boltzman constant, T is temperature, q is elementary charge, V is bias voltage, μ is mobility, τ is lifetime, and d is the crystal thickness (0.15 cm). The diffusion and drift distance at −1 V bias voltage cannot cross the whole crystal thickness, but the drift distance can be multiplied with increasing bias voltage (0.249 cm at −3 V).

Overall, electron transport does not limit the device performance, but the difference in electron drift distance under various biases provides the platform for the variable-spectrum responses in this photodetector.

4. If this is a purely photoconductive detector, why then is the current under forward bias (Fig 3c) so much lower? What happens to the EQE spectrum under forward bias? If electron drift is limiting, should the relative sensitivity for UV and NIR light not switch under forward bias?

Our response: Thanks for the reviewer's question. Although the photodetector in this work operates in photoconductive mode, it is not in ohmic contact. The difference in work function introduces a Schottky barrier, which hinders the supplementation of charge carriers. Under the trap-induced charge injection mechanism, the external electrons increase the probability of tunneling into the device. Thus, the current under negative voltage is amplified. Trap-induced photocurrent increasement have been reported in other photodetectors. (*Nat. Nanotech.* **2012**, *7*, 798-802; *Sci. Adv.* **2020**, *6*, eaaw8065)

Photogenerated holes need to drift to the counter electrode when the photodetector operates at a positive voltage. As mentioned above, the relatively lower hole mobility compared to electron mobility suppresses the drift distance of photogenerated holes under positive voltages. As a result, the lower hole mobility gives rise to the drop of EQE under positive voltages (Figure R10), compared to that of negative voltages. Based on the explanation of the drift distance in the response to Question 2, the lower mobility makes it more difficult to collect UV and infrared carriers at the surface.

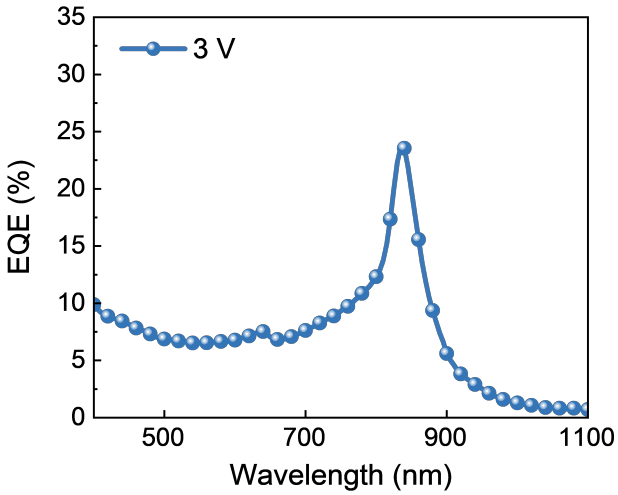

Figure R10. The EQE results of perovskite single crystal photodetector under 3 V bias.

5. The LDR is claimed to be 177 dB. But Fig. 4b clearly shows a roll-off at the highest intensities. A double logarithmic plot hides many of the nonlinearities. It is better to make a semi-logarithmic plot of the ratio of the current and the light intensity versus the log of the light intensity. That should give a horizontal line and any deviation from that is the end of the LDR.

Our response: We believe that there is a misunderstanding here. In the previous figure, the last point at high optical power in the LDR results was to demonstrate photocurrent saturation, that is, deviation from linear relationship at this intensity. This data point is not part of the LDR calculation of 177 dB. To avoid ambiguity, we removed the last data point in the revised figure for LDR results (Figure R11). For the LDR calculation, the double logarithmic graph is currently the most widely applicable method and is adopted by various groups, which helps to compare with other studies. (*Nat. Photon.* **2024**, *18*, 236–242; *Nat. Photon.* **2023**, *17*, 1047–1053; *Nat. Commun.* **2023**, *14*, 5352; *Nat. Commun.* **2023**, *14*, 6935)

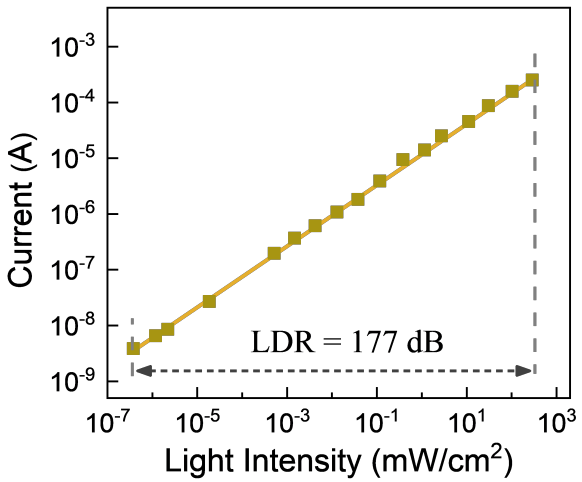

Figure R11. LDR of the photodetector measured at −1 V under 635 nm laser illumination.

6. The time and fall times are relative long. A Si detector is much faster, does that have any consequences for the envisioned applications. Also in Fig. 4e it would be good to also indicate where state-of-the art perovskite photodiodes are positioned. I think LDRs will be similar and rise times well below 1 microsecond.

Our response: We are grateful to the Referee for bringing this interesting detail to our attention. Although the response speed of the perovskite single-crystal detector in the paper is not comparable to the optimal level of response speed of silicon-based detectors, it completely meets the application scenarios mentioned in this manuscript. For example, in 720P security surveillance cameras, the video recording frame rate is generally 25 fps (frame per second), and the number of scan lines is 720. The camera reads signals line by line for each frame, and only records the next frame after all lines have been read. Therefore, strict requirements are only placed on the rise time of the photodetectors. The response time requirement for a single pixel can be estimated by:

$$t_{frame} = \frac{1}{25} = 40\ ms$$

$$t_{line} = \frac{40}{720} = 55.56\ \mu s$$

where t_{frame} is the time required for imaging each frame and t_{line} is the time required for scanning each line. Since the pixels in each line read data synchronously, the t_{line} is the time required for a single pixel. As estimated above, the rise time should be within 55.56 μs, while the descent time requirements are more lenient. Fortunately, the rise time of our perovskite single crystal detector (34.7 μs) satisfies the demand. In addition, after optimizing the interfaces and electrodes of the perovskite single crystal detectors, the response speed can be further improved to reach the level of silicon-based detectors.

We agree with the Referee that perovskite photodiodes based on thin films can retain similar LDRs but show reduced rise times. However, there are two main reasons for choosing perovskite single crystal for comparison in Figure 4e. Firstly and most importantly, the realization of a bias-switchable spectral response from visible to near-infrared region requires gradient distribution of Pb−Sn alloying in space. In theory and practice, thick perovskite films are needed for constructing day/night imaging, which inevitably prolongs the carrier transit time. Secondly, the single-crystal perovskite exhibits enhanced thermal and environmental stability compared with the polycrystalline counterpart due to the absence of grain boundaries in the single crystal (Supplementary Figs. 22 and 36). In addition, perovskite single crystals exhibit much enhanced carrier mobility. Of course, further thinning the single crystal to a thickness of less than 100 μm enables both efficient electronic charge collection and stability improvement. Nevertheless, the crystal growth of thin perovskite single crystals with metal alloying has not yet been well understood, and this will be further developed in future works.

7. A minor issue: In the introduction the authors argue that application of existing ICR devices may be limited by insufficient long-term reliability under harsh conditions. The authors do not compare their single-crystal photodetectors to this statement.

Our response: Thanks to the reviewer for pointing out the issue of not revealing the advantages of photodetectors in this work. Currently, in ICR devices used for day and night imaging, there is an electric filter-switching mechanism. However, the required increase in the number of mechanical components is

undesirable for applications in which a small, lightweight, and highly robust system is necessary, such as in vehicle or drone cameras. Moreover, the motor of the power mechanism itself may be damaged, or the filter cannot be smoothly switched after high load operation.

In contrast, the detector shown here can adjust the detection spectrum by changing the bias voltage, so there is no need for filter-switching devices in the imaging system. Therefore, there are no reliability problems described above. Following the suggestion of the reviewer, we have added descriptions to the manuscript to illustrate the advantages of our photodetector.

REVIEWER COMMENTS

Reviewer #1 (Remarks to the Author):

The author has responded to the reviewer's comments, but the response does not meet the usual academic standards for P2P response and manuscript revision. The responses are extensive but lack specific references to the revised sections of the manuscript (Page and line), making it difficult for reviewers to trace the changes. Despite lengthy explanations, the modifications in the manuscript, marked in red, appear minimal, which is concerning given that the original manuscript contained numerous misleading discussions and interpretations. Upon having a fresh look at the key aspects of the paper:

• The explanation of how the Sn gradient influences the LDR remains unclear, lacking a logical foundation for the observed significant improvement in LDR compared to previous studies.

• The newly added methods section on LDR measurement is missing critical details, such as the types of sensors or probes used alongside the power meter, and whether light power was modulated by turning it on and off for each power.

• The similarity in LDR at wavelengths of 7xx nm and 9xx nm is noted, but without reporting the slope of the current versus power plot, which is crucial for assessing responsivity differences given the variations in wavelength and EQE.

More importantly, there are still critical issues in the revised schematics in Figure 3:

• In panel d, the notion that charge carriers can move in the flatband region after overcoming the injection barrier is physiologically implausible.

• The rationale behind the transport of injected carriers across the device is unclear, especially when considering why excited electrons are not transported similarly.

• The distinction between the transport mechanisms at 700 nm and 900 nm needs clarification. It is suggested that at 900 nm, the mechanism is injection-limited at the interface, whereas at 700 nm, it involves bulk transport of photogenerated carriers. This distinction seems unlikely without supportive evidence.

• Contradictions are also evident between panels a and d of Figure 3, where different mechanisms are proposed for carrier transport: in panel a, the mechanism is focused on the transport of photogenerated carriers; In panel d, the mechanism is shown to be the injection-limited (photoconductive).

To elucidate the underlying mechanisms, I recommend:

• Measuring and reporting the IV curve under 9xx nm illumination, a crucial piece of missing data.

• Recording and detailing the EQE at positive biases, such as +1V and +3V, where significant photocurrent has been reported in the illuminated IV.

• Conducting simple simulations with software like SCAPS, SETFOS, and COMSOL to investigate the mechanisms.

Reviewer #2 (Remarks to the Author):

Comments:

The author provided a detailed response according to the comments. The revised manuscript is more acceptable. Therefore, the revised manuscript can be recommended for publication, but the author still needs to address some questions.

1. The author still should emphasize the innovation of this article in the introduction:

preparing narrow bandgap single crystals and preparing adjustable spectral responses. Otherwise, it may cause misunderstandings among readers.
2. This response is satisfactory.
3. This response is satisfactory.
4. Do single crystals have corresponding disadvantages, such as in terms of response speed? What are the problems that need to be solved in the future?
5. The author should change the expression: Aside from the complicated fabrication techniques, cause the preparation methods reported in many literatures are not complex, some of them are even easier than perovskite single-crystal.
6. I think the spectrometers reported in the literature can also be applied to imaging. But the limitations of the spectrometer proposed by the author do exist.
7. Please check and unify the font in all image.

Reviewer #3 (Remarks to the Author):

The authors have adequately addressed all of my comments and concerns. I recommend publication of this work in Nature Communications.

Reviewer #1 (Remarks to the Author):

The author has responded to the reviewer's comments, but the response does not meet the usual academic standards for P2P response and manuscript revision. The responses are extensive but lack specific references to the revised sections of the manuscript (Page and line), making it difficult for reviewers to trace the changes. Despite lengthy explanations, the modifications in the manuscript, marked in red, appear minimal, which is concerning given that the original manuscript contained numerous misleading discussions and interpretations. Upon having a fresh look at the key aspects of the paper:

1. The explanation of how the Sn gradient influences the LDR remains unclear, lacking a logical foundation for the observed significant improvement in LDR compared to previous studies.

Our Response: Thank you for the suggestion. In the revised manuscript, we refined the discussion on the reasons for the LDR improvement. The improvement of LDR is mainly attributed to three reasons.

The first reason is that the high quality of the perovskite single-crystal leads to a low trap density of crystal bulk, as demonstrated by the SCLC test in the supplementary information and the DLCP test in the main text. The defect states introduced by Sn enrichment only exist in the thin region on the surface, which poses a relatively small impact on the overall defect state density of the crystal. Thus, the bulk charge carriers with long lifetimes are beneficial for the collection efficiency at high carrier concentrations. (*Science* 2015, 347, 519-522; *Nat. Photon.* 2016, 10, 333–339; *Nat. Photon.* 2022, 16, 575–581)

The second reason is that the addition of Pb-Sn alloying can increase carrier mobility, which has been proven by the SCLC test. At the same time, other research has also found that Sn doping can improve the mobility of perovskite devices. The increase in carrier mobility also contributes to the collection of charge carriers. (*Nat. Mater.* 2023, 22, 216–224)

The third reason is that Sn gradient doping introduces an internal electric field, which assists in the collection of charge carriers and reduces the negative impact of surface recombination centers on LDR. (*Nature* 2020, 583, 790–795; *Adv. Mater.* 2022, 34, 2107729)

2. The newly added methods section on LDR measurement is missing critical details, such as the types of sensors or probes used alongside the power meter, and whether light power was modulated by turning it on and off for each power.

Our Response: Thank you for the Reviewer's suggestions. We have further supplemented the details of the LDR measurement method.

Using 635 nm and 940 nm lasers as light sources with constant power, we adjusted the irradiation light intensity on the device by adding different neutral density filters in the optical path. A wide range of optical power adjustments can be achieved by combining filters with varied optical densities (ODs) of 0.5, 1, 3, and 4. After adjusting the filter combination, the actual irradiation

light intensity was further checked using the Newport 843-R optical power meter and the Newport 918D photodiode sensor. Keysight B2901A sourcemeter was used to record the photocurrent of the photodetector. The photodetector operated at −3 V and −1 V bias when tested at 940 and 635 nm, respectively.

3. The similarity in LDR at wavelengths of 7xx nm and 9xx nm is noted, but without reporting the slope of the current versus power plot, which is crucial for assessing responsivity differences given the variations in wavelength and EQE.

Our Response: The LDR data is mainly used to characterize the linear dynamic range between the photocurrent output by the photodetector and the incident light power density, thereby demonstrating the range of light intensity that the device can linearly respond to. We found that the LDR slopes of the perovskite single-crystal photodetector under short-wavelength and long-wavelength laser illumination are both close to 0.56. This kind of slope is due to the presence of trap states at the top surface, which has been reported in many literatures with gain brought by the trap state. (*Nat. Commun.* 2023, 14, 6935, *Nat. Photon.* 2023, 17, 1047–1053, *Adv. Mater.* 2021, *33*, 2008080)

4. More importantly, there are still critical issues in the revised schematics in Figure 3: 4.1 In panel d, the notion that charge carriers can move in the flat band region after overcoming the injection barrier is physiologically implausible.

Our Response: Thank you for the reviewer's comments. In Figure 3d, we emphasize the changes in the Schottky barrier under dark and light conditions, thereby highlighting the mechanism of trap-induced external charge injection. We apologize for not showing the tilt of the energy band under bias voltage, which led to the misunderstanding of carrier movement in the flat band. Following the suggestion from the Referee, we have redrawn Figure 3d (Figure R1) to demonstrate the correct band structure of the photodetector under operation.

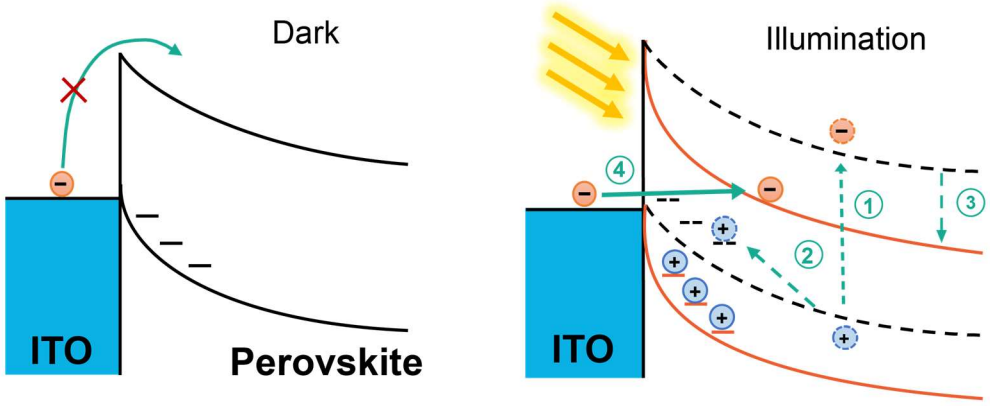

Figure R1. Schematics of the energy band structure under dark and illumination.

4.2 The rationale behind the transport of injected carriers across the device is unclear, especially when considering why excited electrons are not transported similarly.

Our Response: There is no essential difference in the carrier transport mechanism across the device between externally injected carriers and photo-excited carriers. In contrast, the concentration of recombination centers in different regions affects the overall performance of carrier transport (Figure R2).

In the Pb-Sn alloyed perovskite single crystal photodetector, long-wavelength carriers are only generated in the surface tin-rich region, where the oxidized Sn^{4+} leads to severe non-radiative recombination of charge carriers. Therefore, the severe recombination will hinder electron collection by the opposite electrode under low bias voltage. Correspondingly, the lifetime of trapped holes is also significantly reduced by the trap-assisted recombination. In contrast, short-wave carriers generated in the bulk (tin-trace) region inside the crystal have a much longer lifetime since the defect density is much lower than that on the top surface (as shown in Figure 3e). Thereby, even under low bias voltage, electrons could reach the counter electrode.

Under high bias voltage, the drift distance of long-wavelength photo-generated carriers on the surface is enhanced, allowing electrons to drift out of the surface tin-rich region before recombination. Due to the much lower defect density in the bulk, the electrons that drifted into the bulk (tin-trace) region have a longer lifetime, thereby increasing the collection efficiency of excited electrons. After the effective collection of electrons, the lifetime of trapped holes is also significantly extended, resulting in effective trap-induced electron injection. Similarly, the charge carriers injected into the device can quickly drift out of the tin-rich region under high bias voltage, showing the improvement of the collection efficiency.

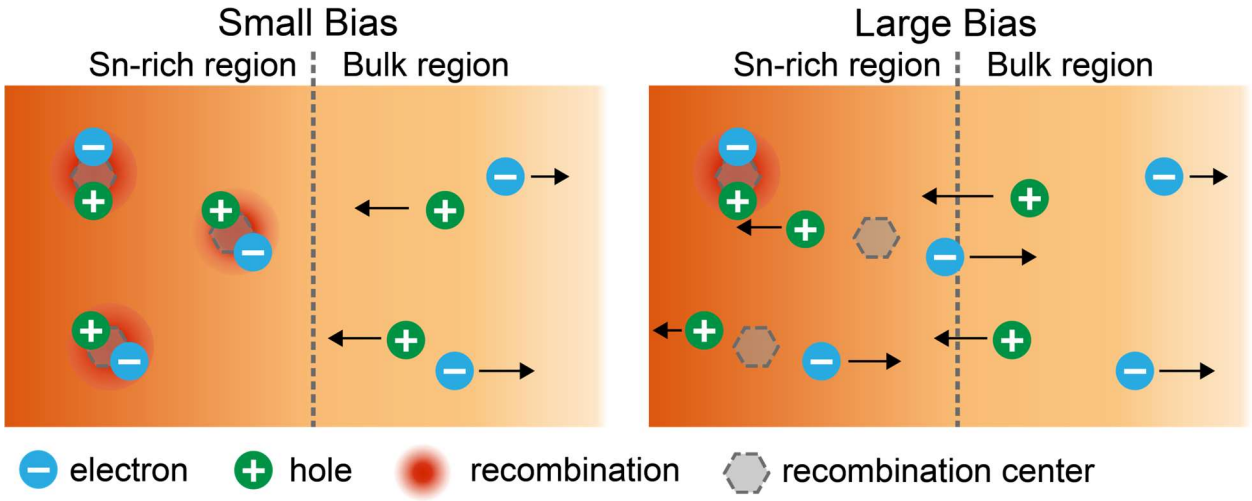

Figure R2. Schematic diagrams of the carrier dynamics under different biases in the regions with different recombination center densities.

In summary, the high defect density in the surface tin-rich region reduces the carrier lifetime,

thereby affecting the transport and collection of long-wavelength photo-generated carriers under low bias voltage. Based on the comments of the Reviewer, we have provided a comprehensive explanation of the working mechanism in the main text.

4.3 The distinction between the transport mechanisms at 700 nm and 900 nm needs clarification. It is suggested that at 900 nm, the mechanism is injection-limited at the interface, whereas at 700 nm, it involves bulk transport of photogenerated carriers. This distinction seems unlikely without supportive evidence.

Our Response: As mentioned above, the main difference between the transport mechanisms of 700 nm and 900 nm lies in the recombination probability at the region where the charge carrier is generated.

900 nm (long-wavelength) light only generates carriers in the surface tin-rich region, where the defect density is over three orders higher than the bulk region of the crystal. Under low bias voltage, carriers with short carrier lifetimes easily undergo recombination before leaving the region. Under high bias voltage, electrons have more chances of leaving the tin-rich region before recombination. In such a case, the bulk region with extremely low defect density enables the drifted electrons to reach the counter electrode. Furthermore, the decrease in electron concentration prolongs the lifetime of trapped holes. As a result, the trapped holes induce band bending, narrow the Schottky barrier, and increase the injection of external electrons.

In contrast, 700 nm light can be absorbed in both tin-rich and tin-trace regions, generating electron-hole pairs. The carriers generated in the tin-rich surface region are similar to those of 900 nm, while the long-lived carriers in the tin-trace bulk region can be transported and collected under small bias voltages.

Therefore, 700 nm and 900 nm light exhibit different response results under small bias voltages. Based on the comments of the Reviewer, we have supplemented the explanation of the mechanism.

4.4 Contradictions are also evident between panels a and d of Figure 3, where different mechanisms are proposed for carrier transport: in panel a, the mechanism is focused on the transport of photogenerated carriers; In panel d, the mechanism is shown to be the injection-limited (photoconductive).

Our Response: When the device is operating, the mechanism of Figure 3a and 3d is coexistence. Figure 3a mainly elaborates on the light absorption of different wavelengths and the position of charge carrier generation, as well as the relationship between electron drift distance and collection efficiency under different bias voltages. Figure 3d mainly illustrates the trapping effect on holes, thereby bending the energy band and increasing the tunneling probability of external electrons.

As stated in the responses to questions 4.2 and 4.3, different recombination center densities in absorption regions affect the lifetime of photo-generated carriers of different wavelengths, thereby

affecting the drift distance. The device changes in response to different wavelengths at different biases under the mechanism described in Figure 3a, while some holes are trapped and amplified in response performance under the mechanism described in Figure 3d.

5. To elucidate the underlying mechanisms, I recommend:

5.1 Measuring and reporting the IV curve under 9xx nm illumination, a crucial piece of missing data.

Our Response: In Supplementary Figure 27, we compared dark current, photocurrent under white light, and photocurrent under 940 nm light in linear coordinates. In the analysis of the main text, we discussed the relationship between the opening voltage of photocurrent under 940 nm light and the EQE curve under different biases, and once again demonstrated our proposed response mechanism. Based on the reviewer's suggestions, we further discussed the photocurrent under 940 nm illumination in the main text.

5.2 Recording and detailing the EQE at positive biases, such as +1V and +3V, where significant photocurrent has been reported in the illuminated IV.

Our Response: Thanks for the reviewer's suggestions. We conducted EQE measurement under positive bias in the supporting material and added the discussion in the main text. Under positive voltage, the charge carriers that need to pass through the entire crystal are holes rather than electrons. Since the mobility of holes is much lower than that of electrons, long wavelength photo-generated carriers are more difficult to collect and the overall EQE spectra are smaller than those of under negative voltages (Figure R3).

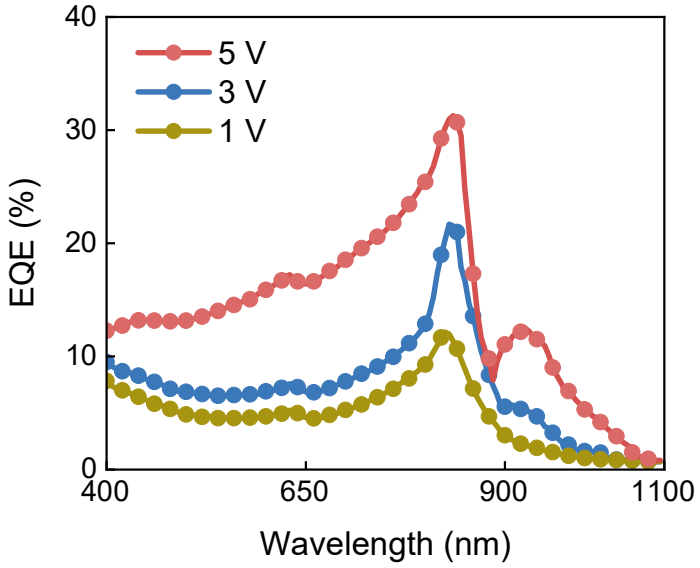

Figure R3. The EQE spectra of the perovskite single crystal photodetector measured at different positive biases.

5.3 Conducting simple simulations with software like SCAPS, SETFOS, and COMSOL to investigate the mechanisms.

Our Response: Based on the reviewer's suggestions, we conducted a mechanism study on the simplified model of the device using COMSOL. We set up perovskite layers doped with different Sn concentrations based on the measured optical and electrical parameters. We calculated the quantum efficiency of short-wavelength light and long-wavelength light under different bias voltages to verify the response changes.

The simulated external quantum efficiency (EQE) results of the photodetector are shown in Figure R4a. Under −1 V bias, the device produces almost no photocurrent under 940 nm light irradiation compared to a distinct EQE signal under 750 nm light irradiation, which is consistent with the actual results. As the bias voltage increases, the EQE values at 750 nm and 940 nm both gradually increase. Notably, the EQE value at 940 nm under −3 V bias is much higher than that of at 750 nm light under −1 V bias, which is also consistent with the actual test results.

To demonstrate the changes in EQE, we present the ratio of EQE at 940 nm to EQE at 750 nm under different bias voltages in Figure R4b. When the device operates at −1 V, there is almost no response to 940 nm light and the EQE ratio is relatively low with a value of approximately 0.02. As the bias voltage increases, even though the EQE at 750 nm increases, the response of the device to 940 nm light changes more significantly and the ratio gradually increases to over 0.85. This is consistent with the actual measurement, in which the EQE ratio increases from approximately 0.05 to approximately 0.9.

Overall, the simulation results support the proposed mechanisms of the carrier dynamics in the Pb−Sn perovskite device under different biases.

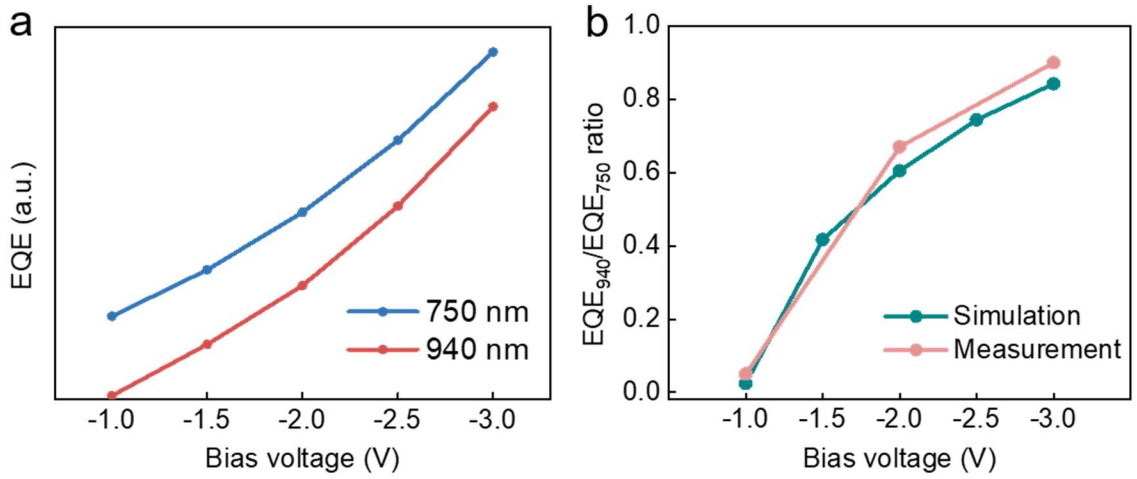

Figure R4. (a) Simulation EQE results of photodetectors at different wavelengths. a, The relationship between EQE of different wavelengths and bias voltage. (b) The dependence of the EQE ratio between 750 nm and 940 nm on voltage.

Reviewer #2 (Remarks to the Author):

Comments:
The author provided a detailed response according to the comments. The revised manuscript is more acceptable. Therefore, the revised manuscript can be recommended for publication, but the author still needs to address some questions.

Our Response: We thank the Referee for the positive comments on our work and the revised changes.

1. The author still should emphasize the innovation of this article in the introduction: preparing narrow bandgap single crystals and preparing adjustable spectral responses. Otherwise, it may cause misunderstandings among readers.

Our Response: Given the Reviewer's comment, we have now rewritten the second paragraph of Introduction section and highlight the innovation of this article.

2. This response is satisfactory.

Our Response: We are very delighted that the Reviewer feels satisfied with the revised changes.

3. This response is satisfactory.

Our Response: We are very delighted that the Reviewer feels satisfied with the revised changes. These remarks helped us improve the discussion and clarify the critical points within the experimental observation.

4. Do single crystals have corresponding disadvantages, such as in terms of response speed? What are the problems that need to be solved in the future?

Our Response: We thank the referee for this comment. We agree with the Review that the fast response speed is also a critical parameter for the practical application of photodetectors for image application. Perovskite single crystals exhibit a largely suppressed density of those structural defects due to the ordered lattice arrangement, demonstrating their excellent stability and charge mobility compared to their polycrystalline thin-film counterparts. Thus, the perovskite single-crystal photodetectors usually show high responsivity and specific detectivity. However, perovskite single-crystal photodetectors always exhibit a longer response time than that of other low-dimensional materials, which is mainly caused by the ion shielding effect and the too-large thickness of the bulky crystals. (Adv. Sci. 2021, 8, 2100569) Since current methods to grow millimeter-sized perovskite single-crystal thin films usually lead to a crystal thickness of larger than 10 μm, reducing the crystal thickness can effectively increase the device response speed. (*Nat Photonics* 2015**,** *9* (10), 679-686; Adv. Mater. 2017, 29, 1703209) Thus, developing a novel

method to further reduce the crystal thickness to be comparable to the polycrystalline thin film is an urgent question to be solved, which will benefit the development of photodetectors with sub-nanosecond response time. Besides, reducing the crystal thickness will lead to an obvious increase in the device capacitance, and thus result in the resistance-capacitance (RC) constant, which conflicts with the reduced transit time. Therefore, these two factors should be considered simultaneously to achieve the sub-nanosecond response time. In the revised manuscript, we have already emphasized this prospect of response speed.

5. The author should change the expression: Aside from the complicated fabrication techniques, cause the preparation methods reported in many literatures are not complex, some of them are even easier than perovskite single-crystal.

Our response: We agree with the Referee that the description of complicated fabrication techniques is not exactly accurate. Since we rewrote the Introduction, this description is no longer in the revised manuscript.

6. I think the spectrometers reported in the literature can also be applied to imaging. But the limitations of the spectrometer proposed by the author do exist.

Our response: We agree with the Reviewer that some miniaturized spectrometers can also be applied to spectral imaging. (*Nat. Photonics* 2021, 15, 601–607) We agree that there are greatly limitation differences between spectrometer and imaging. As we know, spectrometers are constructed to provide a highly accurate calibrated wavelength and light level reading provided the signal is strong enough across the full spectrum that is to be measured. In contrast, optical imaging uses red, green, and blue colors through a detector array to obtain detailed images. Again, we want to emphasize that the key significance of the paper is developing perovskite single-crystal photodetectors for day/night imaging without the mechanically retractable Infrared Cutfilter Removal (ICR).

7. Please check and unify the font in all image.

Our response: All the font in the images have been checked and unified now.

REVIEWER COMMENTS

Reviewer #1 (Remarks to the Author):

The submitted manuscript entitled “Day/Night Imaging without Infrared Cutfilter Removal based on Metal-Gradient Perovskite Single Crystal Photodetector” has been improved through the revision. I have two minor comments:

- The details of the COMSOL simulation should be added to the Methods section. All parameters used for the simulation, including device architecture, mobility, absorption coefficients, trap densities, and layer thicknesses, should be included. This section should also present the simulated dark and illuminated IV characteristics for the studied wavelength.

- The IV curves in SI Figure 28 should be shown on a logarithmic scale. As this data is very important, the illuminated IV curve under 940 nm light should be included in the main text as Figure 3c.

Reviewer #2 (Remarks to the Author):

This revised version can be accepted now.

Reviewer #1 (Remarks to the Author):

The submitted manuscript entitled “Day/Night Imaging without Infrared Cutfilter Removal based on Metal-Gradient Perovskite Single Crystal Photodetector” has been improved through the revision.

Our response: We thank the Review for the positive assessment of our updated manuscript.

I have two minor comments:

1. The details of the COMSOL simulation should be added to the Methods section. All parameters used for the simulation, including device architecture, mobility, absorption coefficients, trap densities, and layer thicknesses, should be included. This section should also present the simulated dark and illuminated IV characteristics for the studied wavelength.

Our Response: Thank you for the suggestion. We have added the simulated dark and illuminated IV characteristics in Supplementary Figure 25 (Figure R1) and the description in the Results and discussions section on Page 11 (lines 270−272) of the main manuscript. In addition, we supplemented the key parameters used for COMSOL simulation in Table R1, which has been added to Supplementary Table 4.

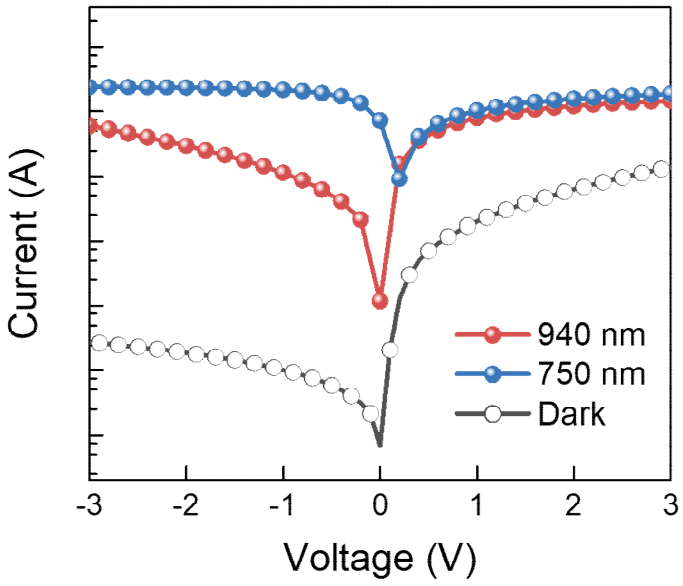

Figure R1. Simulation IV characteristics at dark and under illumination of 750 and 940 nm light.

Table R1. Key parameters used for perovskite photodetector simulation.

Layer[a]	1	2	3	4	5
Perovskite	Sn enriched	Sn enriched	Sn enriched	Sn enriched	bulk
Thickness (nm)	30	30	30	30	5×10^{5}
μ_n ($cm^2V^{-1}s^{-1}$)	293	293	293	293	293
μ_p ($cm^2V^{-1}s^{-1}$)	23.7	23.7	23.7	23.7	23.7
Trap density (cm^{-3})[b]	1×10^{19}	1×10^{17}	1×10^{15}	1×10^{13}	1×10^{12}
k_{750}	0.273	0.259	0.256	0.255	0.255
k_{940}	0.202	0.062	0.028	0.018	0.012

[a]We set up perovskite layers doped with different Sn concentrations based on the measured optical and electrical parameters. Layers 1-4 are surface Sn-rich regions (from the outside to the inside) with a thickness of 30 nm for each layer. Layer 5 is the bulk region with a thickness of 500 μm.
[b]Derived from the results of DLCP.

2. The IV curves in SI Figure 28 should be shown on a logarithmic scale. As this data is very important, the illuminated IV curve under 940 nm light should be included in the main text as Figure 3c.

Our Response: According to the reviewer's comments, we have added the logarithmic scale IV curve under 940 nm illumination to Figure 3c (Figure R2) and revised the discussion in the Results and discussions section on Page 11 (lines 269−271) of the main manuscript. In addition, as the logarithmic scale infrared IV curve is shown in Figure 3c, we have retained the linear scale IV curve in Supplementary Figure 28 to facilitate the understanding of the changes in current at different wavelengths.

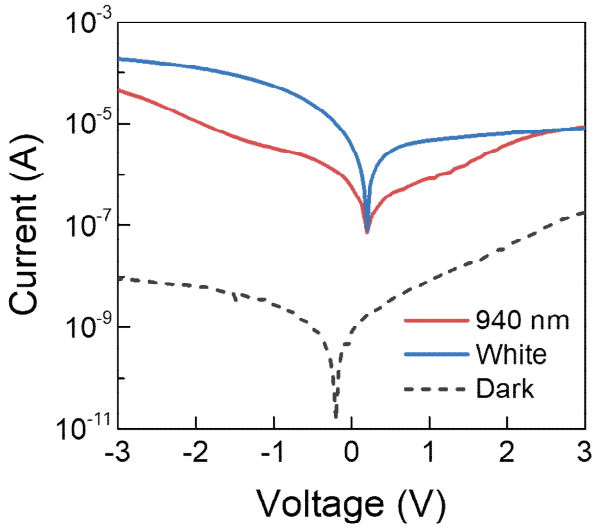

Figure R2. Current-voltage curves of the perovskite photodetector under dark and (white and 940 nm light) illumination conditions.

Besides, in the confidential remark, Reviewer #1 expressed that the response letter again failed to follow the standard practice, as they pointed out in the last round of assessment.

Our Response: Thank you for the suggestion. In the previous version of the revision, we have only highlighted the change in a different color (red). To make it easier for the Reviewers to trace the changes, we have clarified which line and page we have revised based on the Reviewer's suggestion in this revision.

Reviewer #2 (Remarks to the Author):

This revised version can be accepted now.

Our Response: We thank the Reviewer for the positive comments on the work.

REVIEWERS' COMMENTS

Reviewer #1 (Remarks to the Author):

The authors have provided the requested data, and I have no further comments.